NJC

Accepted Manuscript

This is an *Accepted Manuscript*, which has been through the Royal Society of Chemistry peer review process and has been accepted for publication.

Accepted Manuscripts are published online shortly after acceptance, before technical editing, formatting and proof reading. Using this free service, authors can make their results available to the community, in citable form, before we publish the edited article. We will replace this *Accepted Manuscript* with the edited and formatted *Advance Article* as soon as it is available.

You can find more information about *Accepted Manuscripts* in the Information for Authors.

Please note that technical editing may introduce minor changes to the text and/or graphics, which may alter content. The journal's standard Terms & Conditions and the Ethical guidelines still apply. In no event shall the Royal Society of Chemistry be held responsible for any errors or omissions in this *Accepted Manuscript* or any consequences arising from the use of any information it contains.

ROYAL SOCIETY OF CHEMISTRY

www.rsc.org/njc

Journal Name

RSCPublishing

COMMUNICATION

A Narrow Band Gap Isoindigo Based Molecular Donor for Solution Processed Organic Solar Cells

Cite this: DOI: 10.1039/x0xx00000x

Jetsuda Areephong,[a] Ronan R. San Juan,[a] Abby-Jo Payne [a] and Gregory C. Welch[a*]

Received 00th January 2012,
Accepted 00th January 2012

DOI: 10.1039/x0xx00000x

www.rsc.org/

The synthesis and characterization of a novel isoindigo based small molecule semiconductor is reported. The new compound exhibits broad and efficient optical absorption extending beyond 800 nm, relatively low lying HOMO and LUMO energy levels of -5.14 and -3.69 eV, respectively, and good solubility in common organic solvents. When paired with $PC_{61}BM$, organic solar cells gave power conversion efficiencies as high as 3.2%, among the highest achieved for small molecule isoindigo based systems.

Isoindigo is an organic pigment that has recently found utility as a useful building block to construct high performance organic semiconductors.[1–3] The pigment is easily synthesized from low-cost feed stocks, is electron deficient, and can be readily functionalized with solubilizing alkyl side chains making it an ideal acceptor within the context of donor-acceptor (D-A) type organic materials. Isoindigo based conjugated polymers have been used as donor components in organic solar cells (OSCs) with power conversion efficiencies above 7%[4], and as hole and electron transporting materials in high mobility thin film transistors.[5–8] Isoindigo based small molecules, on the other hand, have been far less studied. Reynolds reported the first soluble small molecule systems based upon isoindigo in 2010.[9] When used as donors in bulk heterojunction (BHJ) OSCs, maximum power conversion efficiencies (PCEs) of 1.76% were achieved. These early systems were prone to crystallization into large domains unsuitable for efficient charge separation, but through rigorous processing optimization, PCEs were improved to 3.2%.[10] Subsequently, Lee[11] and Loo[12] have developed novel isoindigo based small molecule donors and have reported OCSs with PCEs of ~ 3%. Several other isoindigo based small molecule donors have been reported, but all with device PCEs below 3%.[13–17] We have recently developed isoindigo small molecules for use as acceptors in BHJ solar cells.[18] Continuing our development of isoindigo based small molecules, we became interested in incorporating isoindigo into one of the best performing donor architectures for OSCs which has been reported to give PCEs of 6-9%.[19–22] In this contribution we report on the synthesis, characterization, and photovoltaic properties of a donor-acceptor-donor-acceptor-donor (DADAD) based small molecule using isoindigo as the 'A' unit. When paired with $PC_{61}BM$, BHJ OSCs with PCEs of 3.2% were realized.

The chemical structure of the target compound, identified as $DTS(IIThTh_{HEX})_2$, is shown in Figure 1. The structure consists of a dithienylsilole (DTS) core flanked with isoindigo (II) units and end-capped with hexyl bithiophene ($ThTh_{HEX}$) moieties. The DTS core and $ThTh_{HEX}$ end-cap have been widely used to construct high performance molecular donors.[19,23,24] It was found that substitution of butyl alkyl chains onto the II units provided $DTS(IIThTh_{HEX})_2$ with sufficient solubility in common processing solvents (e.g. dichloromethane, chloroform, xylenes, and chlorobenzene) to ensure purification by column chromatography and uniform film formation by solution deposition, the latter a prerequisite for OSC device fabrication. $DTS(IIThTh_{HEX})_2$ was synthesized using standard synthetic methods.[25] Full details on synthesis and spectroscopic characterization can be found in the supporting information. It is noteworthy to mention that the mono-functionalization of dibrominated isoindigo via Stille cross-coupling procedures proceed in high yield (>60%) using conventional heating, whereas using the popular microwave irradiation technique gave considerably lower yields (<30%) of the desired product.

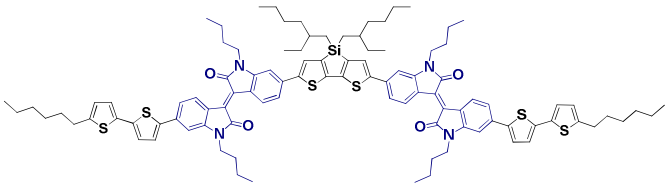

Figure 1. Chemical structure of the small molecule $DTS(IIThTh_{HEX})_2$ synthesized in this study. The key isoindigo (II) unit is highlighted in purple.

Critical to the operation of OSCs is the ability of the active BHJ layer to efficiently absorb light. Fullerene based OSCs require the donor component to be primarily responsible for light absorption, with absorption in the region from 300-800 nm being desirable. The optical absorption of DTS(IIThTh$_{HEX}$)$_2$ was measured in both the solution and solid state using solvents with both relatively high (chloroform) and low (xylenes) vapour pressure. Chloroform is a common solvent used for solution processed OSC, whereas xylenes is becoming more popular owing to its lack of halogen atoms making it a 'greener' solvent.[26,27] Optical absorption profiles are shown in Figure 2.

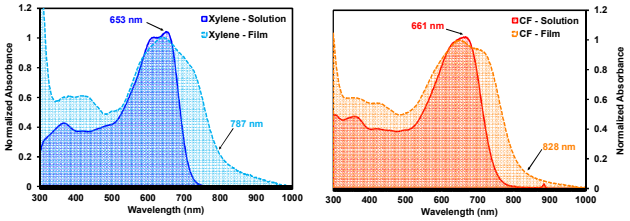

Figure 2. Optical absorption profiles of the small molecule DTS(IIThTh$_{HEX}$)$_2$ in solution (solid lines) and as as-cast spin coated films (dashed lines). Left plot (blue traces) use xylenes as solvent. Right plot (red traces) use chloroform as the solvent.

In xylenes, DTS(IIThTh$_{HEX}$)$_2$ exhibits an absorption onset (λ_{onset}) at 732 nm and a strong absorption maximum (λ_{max}) at 653 nm (ε = 139,000 $M^{-1}cm^{-1}$). In chloroform solution, a redshift in both λ_{onset} and λ_{max} to 772 and 661 nm (ε = 175,000 $M^{-1}cm^{-1}$) is observed. This bathochromic shift is attributed to stabilization of the charge transfer state in the more polar chloroform solvent. In both cases, the low energy transition is dominant, which is common for linear D-A type systems with extended π-conjugation. Upon transitioning from solution to solid state, a significant redshift in λ_{onset} is observed owing to stronger interchromophore interactions. Interestingly, thin-films cast from chloroform solutions exhibit a slightly higher intensity lowest energy shoulder and a smaller optical band gap (ca. 1.50 eV) when compared to films processed from xylenes (1.58 eV). These results suggest that DTS(IIThTh$_{HEX}$)$_2$ might form a more organized nanostructure when processed from chloroform solution. No significant changes in either absorption profile were observed upon thermal annealing, a common technique to induce morphological changes in the thin-films (Figure S8). Focusing on the absorption profile of the thin-films processed from chloroform solution, DTS(IIThTh$_{HEX}$)$_2$ is clearly capable of photon harvesting from 300-800 nm with strongest absorption from 500-800 nm, ideal for use as a donor component in fullerene based OSCs. Compared to related structures reported in the literature, the λ_{onset} of DTS(IIThTh$_{HEX}$)$_2$ is blue-shifted by 12 nm from a similar molecule using diketopyrrolopyrrole (SiTDPP-EE-C6)[28] in place of isoindigo. On the other hand, it is red-shifted by 28 and 13 nm from small molecules using mono-fluoro benzothiadiazole (DTS(FBTTh$_2$)$_2$)[22] and pyridyl thiadiazole (DTS(PTTh$_2$)$_2$)[21] respectively in place of isoindigo. These changes are minimal and in each case the profiles are similar, reflecting the strong electron accepting ability of each unit. DTS(IIThTh$_{HEX}$)$_2$ was found to be emissive in xylenes with a maximum emission centred at 720 nm.

The electrochemical properties of DTS(IIThTh$_{HEX}$)$_2$ were determined using cyclic voltammetry. The cyclic voltammogram (Figure S9) exhibited two reversible oxidations at 0.55 and 0.91 V and two reversible reductions at -1.28 and -1.60 V. The onset of oxidation and reduction occurred at 0.37 V and -1.14 V, respectively. These values were used to approximate the HOMO (-5.17 eV) and LUMO (-3.66 eV) energy levels. These values are comparable to the related compounds mentioned previously and are appropriately offset from those of $PC_{61}BM$, thus DTS(IIThTh$_{HEX}$)$_2$ is suitable to act as a donor in BHJ OSCs. Interestingly, DTS(IIThTh$_{HEX}$)$_2$ exhibited no melting or crystallization peaks in the range of 100-300°C when evaluated using differential scanning calorimetry (DSC) (Figure S10). This is in stark contrast to SiTDPP-EE-C6, DTS(FBTTh$_2$)$_2$) and DTS(PTTh$_2$)$_2$) which all exhibit distinct melting and crystallization transitions between 150 and 210°C. These results imply that the isoindigo compound is amorphous in the solid state. Indeed, XRD experiments on thin-films cast from both xylenes and chloroform showed no significant diffraction patterns (Figure S11).

Theoretical calculations were used to probe the gas-phase structure, electronic structure, and electronic transitions of DTS(IIThTh$_{HEX}$)$_2$, see ESI for full computational methods. The optimized geometry of DTS(IIThTh$_{HEX}$)$_2$ with truncated alkyl chains is shown in Figure 3a. The dihedral angles between the DTS and II units, and II and Th units, are ~20°, resulting in a π-conjugated backbone that is significantly distorted from planarity. This distortion is a result of steric interactions between the H-atoms on the 6 and 5 membered rings adjacent to one another.

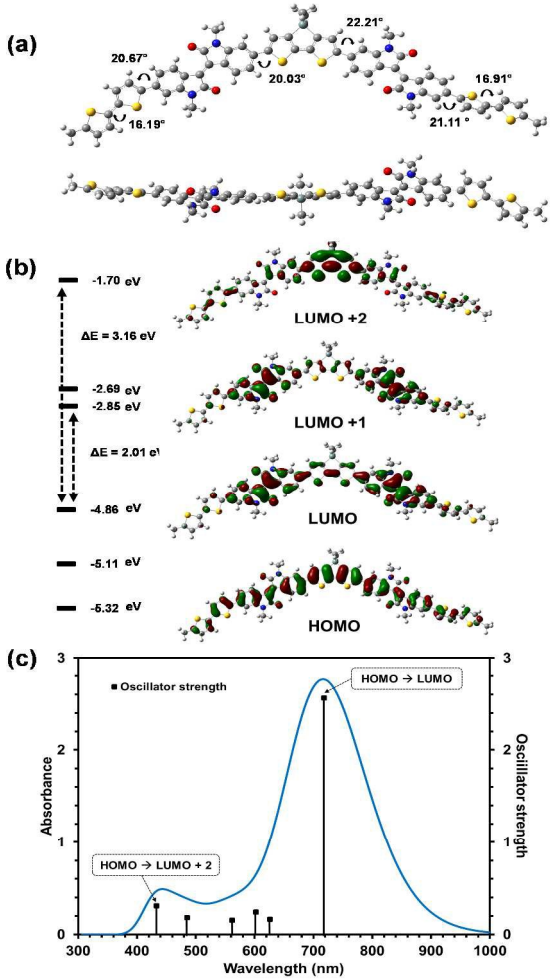

Figure 3. (a) Optimized structure, (b) electronic energy levels and molecular orbital descriptions, and (c) predicted optical absorption spectra of DTS(IIThTh$_{HEX}$)$_2$ with truncated alkyl groups. Calculations carried out in gas-phase using DFT and TD-DFT methods at the B3LYP/6-31G(d,p) level of theory.

A non-planar backbone can inhibit efficient intermolecular π–π stacking in the solid state and may explain the lack of crystallinity observed within the spin-cast films of DTS(IIThTh$_{HEX}$)$_2$. This hypothesis correlates with the observations that the related compounds SiTDPP-EE-C6,[28] DTS(FBTTh$_2$)$_2$,[22] and DTS(PTTh$_2$)$_2$[21,29,30] all have planar structures in the gas-phase and form ordered structures in the solid state. The observed deviation from planarity does not negatively impact the overlap of π-orbitals as both the HOMO and LUMO are mostly delocalized across the molecular backbone (Figure 3b). The predicted optical absorption profile correlates with the observed solution spectra with two primary bands at high and low energies (Figure 3c). The long wavelength absorption band is a result of electron transitions between the HOMO and LUMO, while the short wavelength absorption band is primarily a result of a HOMO to LUMO+2 transition. See Table S1 for a complete list of electronic transitions.

Important to this study was the incorporation of DTS(IIThTh$_{HEX}$)$_2$ into photovoltaic devices. A standard architecture of ITO/PEDOT:PSS/ DTS(IIThTh$_{HEX}$)$_2$:PC$_{61}$BM/Ca/Al was used and we focused on the optimization of the active layer deposition and post-deposition conditions. Control devices based upon a DTS(FBTTh$_2$)$_2$:PC$_{61}$BM active layer were also fabricated to give a relative comparison to our laboratory processing conditions. Complete details on device fabrication and testing can be found in the ESI. Based on the difference observed in the thin film absorption profiles when using different spin-casting solvents, we first investigated active layers processed from xylenes and chloroform with varying DTS(IIThTh$_{HEX}$)$_2$:PC$_{61}$BM weight ratios of 70:30, 60:40, 50:50, 40:60, and 30:70, using thermal annealing as a post-deposition processing technique. Tabulated data, current-voltage plots, and corresponding UV-vis spectra can be found in the supporting information.

Table 1. V_{OC}, J_{SC}, FF and PCE of 50:50 DTS(IIThTh$_{HEX}$)$_2$:PC$_{61}$BM devices cast from 3% wt/v $CHCl_3$ solutions with increasing DIO concentration.

DIO (%)	V_{OC} (V)	J_{SC} (mA cm^{-2})	FF	PCE (%)
0.25	0.696 ± 0.03	3.7 ± 0.1	0.46 ± 0.03	1.16 ± 0.1
1	0.664 ± 0.06	7.7 ± 0.4	0.34 ± 0.03	1.73 ± 0.2
3	0.694 ± 0.009	11.2 ± 0.6	0.40 ± 0.03	3.11 ± 0.2
5	0.686 ± 0.009	11.3 ± 0.6	0.41 ± 0.02	3.19 ± 0.2
7	0.683 ± 0.009	11.3 ± 0.6	0.42 ± 0.04	3.19 ± 0.2
9	0.680 ± 0.005	11.1 ± 0.3	0.41 ± 0.04	3.10 ± 0.3
11	0.610 ± 0.07	10.4 ± 0.3	0.37 ± 0.01	2.32 ± 0.4

1) DIO = Diiodooctane, volume/volume
2) Films were spin-cast at 1500 rpm for 60 seconds
3) All devices measured without any post film-deposition treatment

Of the devices processed from xylenes, an as-cast active layer with a 30:70 D:A ratio gave best results with an open circuit voltage (Voc) of 0.61 V, a short circuit current (Jsc) of 1.38 mA/cm^2, and a fill factor (FF) of 0.48 corresponding to a final PCE of 0.38%. Of the devices processed from chloroform, an annealed active layer (180°C for 5 minutes) with a 50:50 D:A ratio gave the best results with a Voc of 0.73 V, a Jsc of 4.06 mA/cm^2, and a FF of 0.45 corresponding to a final PCE of 1.33%. Considering chloroform gave the best results, we attempted to improve the device PCE by incorporating small amounts of the solvent additive diiodooctane (DIO) into the pre-deposition solution. DIO is one of the most useful additives available to improve the D:A morphology and increase device PCE.[31] Active layers were processed from 3% weight chloroform solutions with a 50:50 D:A ratio with varying amounts (v/v%) DIO added. Results are given in Table 1. Addition of 0.25 v/v% of DIO to the pre-deposition solution resulted in a decrease in PCE to 1.16% due to a lower Jsc. Increasing DIO concentration to 1% increased the Jsc to 7.73 mA/cm^2, improving the PCE to 1.73%. Increasing the amount of DIO to 5% v/v gave best results with a Voc of 0.69 V, a short circuit current of 11.32 mA/cm^2, a fill factor (FF) of 0.40 corresponding to a final PCE of 3.19%. Use of 7% v/v DIO gave same results, while further concentration increases resulted in a decrease in device performance. The PCE of 3.2% is among the best for isoindingo based small molecules, but does fall short of the 6-7% PCE reported for DTS(FBTTh$_2$)$_2$) and DTS(PTTh$_2$)$_2$) using a similar device architecture.[21,22] Most intriguing was that a relatively high volume of DIO solvent additive was required to induce improvements in device performance, as most small molecule systems are quite sensitive to DIO processing, requiring only a small fraction (<1%) of DIO to achieve maximum device performance.[30] The external quantum efficiency was measured for the best performing device (5% DIO) and shows photo-current generation beyond 800 nm. The integrated current density matched the observed within 2%.

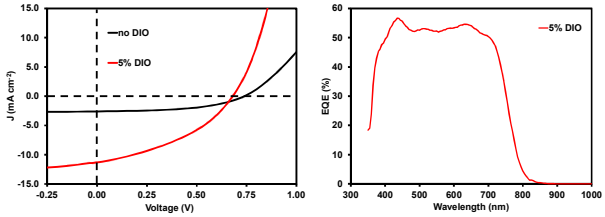

Figure 4. Current voltage plots (left) and external quantum efficiency graph (right) for DTS(IIThTh$_{HEX}$)$_2$:PC$_{61}$BM based organic solar cells. Red trace is for active layer processed from a 3% wt/v chloroform solution (50:50 D:A ratio) with 5% v/v DIO additive. PCE = 3.2%.

To gain insight into the PCE changes upon processing with DIO additive, we probed the active layer microstructure using atomic force microscopy (AFM). Topography images are shown in Figure 4. As shown, increasing the amount of DIO results in increased phase separation of the two active layer components. As-cast films are fairly smooth and uniform. At 5 and 7% DIO (which give best PCE), there is clear phase separation of the two components. Above 7% DIO added the films become quite rough with large aggregated domains. Overall each of the films processed with DIO films exhibit large domains well over 100 nm, which is non-ideal for efficient exciton separation, which plays a factor in the overall lower performance compared to state-of-the-art organic solar cells. Evaluation of the films by X-ray diffraction (Figure S12) showed no significant diffraction peaks at low angles. This is consistent with the inability of DTS(IIThTh$_{HEX}$)$_2$ to undergo melting and crystallization transitions, thereby suggesting that DTS(IIThTh$_{HEX}$)$_2$ cannot form well organized (i.e. crystalline) nanostructures. These observations are in stark contrast to the related compounds SiTDPP-EE-C6, DTS(FBTTh$_2$)$_2$, DTS(PTTh$_2$)$_2$ described previously, which all form crystalline thin-films. Thus, the isoindigo building block appears to impart unique properties on this molecular architecture, which are worth exploring in further detail.

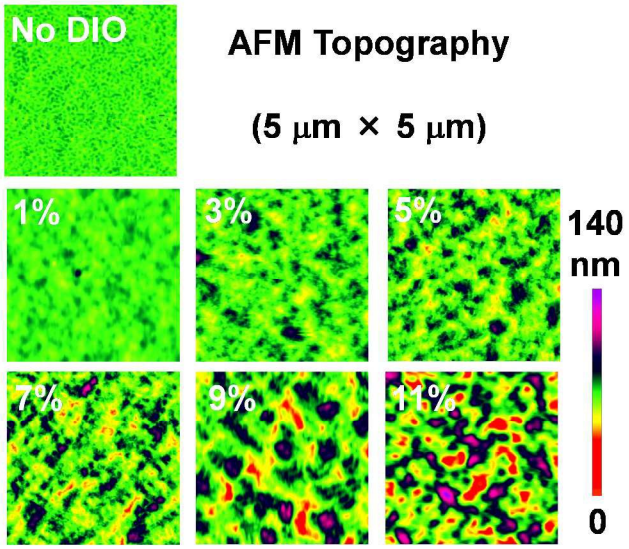

Figure 5. AFM images of DTS(IIThTh$_{HEX}$)$_2$:PC$_{61}$BM active layers processed from chloroform with varying amounts of DIO additive. DIO % is v/v. Actual solar cell devices used to obtain images.

In summary, we have reported on the synthesis and characterization of a novel isoindigo based narrow band gap small molecule, investigated its photo-physical properties and evaluated its utility as a donor component in OSCs. The molecule, DTS(IIThTh$_{HEX}$)$_2$ exhibits broad and efficient absorption extending beyond 800 nm, which is redshifted from related isoindigo small molecules, but similar to high performance materials utilizing DTS cores and ThTh$_{HEX}$ end capping units. The frontier molecular orbital levels were determined to be appropriate for pairing with the fullerene acceptor PC$_{61}$BM. Solution processed BHJ solar cells were found to give a reasonable PCE of 3.2% when the active layer was processed from chloroform solutions containing DIO additive. This value is among the best reported for OSCs using isoindigo based small molecules. The overall PCE appears to be limited by a non-ideal active layer morphology consisting of large domains unfavourable for efficient charge separation. It is expected that through processing and device architecture optimization, along with structure modification, specifically tuning the alkyl chain on the isoindigo fragment, the morphology and corresponding PCE could be improved.

Notes and references

[a] Department of Chemistry Dalhouise University, 6274 Coburg Road, Halifax, Nova Scotia, Canada B3H 4R2.
*corresponding author: gregory.welch@dal.ca

†GCW acknowledges the Canada Research Chairs Program for salary support. AJP is grateful for a Nova Scotia graduate scholarship. Next Energy Technologies is acknowledged for supporting JA and RSJ. Jon-Paul Sun is acknowledged for assistance with EQE measurements. We are grateful to Professor Ian Hill (Dalhousie Physics) for use of his solar device testing equipment and ACEnet for computational resources.

Electronic Supplementary Information (ESI) available: Complete synthetic details, NMR spectra, UV-vis spectra, CV traces, DSC traces, XRD traces, and table of solar cell device parameters. See DOI: 10.1039/c000000x/

1 T. Lei, J.-Y. Wang and J. Pei, *Acc. Chem. Res.*, 2014, **47**, 1117–1126.
2 E. Wang, W. Mammo and M. R. Andersson, *Adv. Mater.*, 2014, **26**, 1801–1826.
3 R. Stalder, J. Mei, K. R. Graham, L. A. Estrada and J. R. Reynolds, *Chem. Mater.*, 2014, **26**, 664–678.
4 C.-C. Ho, C.-A. Chen, C.-Y. Chang, S. B. Darling and W.-F. Su *J. Mater. Chem. A*, 2014. **2**, 8026–8030.
5 P. Deng and Q. Zhang, *Polym. Chem.*, 2014, **5**, 3298–3305.
6 T. Lei, J.-H. Dou, Z.-J. Ma, C.-J. Liu, J.-Y. Wang and J. Pei, *Chem. Sci.*, 2013, **4**, 2447–2452.
7 T. Lei, J.-H. Dou, Z.-J. Ma, C.-H. Yao, C.-J. Liu, J.-Y. Wang and J. Pei, *J. Am. Chem. Soc.*, 2012, **134**, 20025–20028.
8 F. Grenier, P. Berrouard, J.-R. Pouliot, H.-R. Tseng, A. J. Heeger and M. Leclerc, *Polym. Chem.*, 2013, **4**, 1836–1841.
9 J. Mei, K. R. Graham, R. Stalder and J. R. Reynolds, *Org. Lett.*, 2010, **12**, 660–663.
10 K. R. Graham, P. M. Wieruszewski, R. Stalder, M. J. Hartel, J. Mei, F. So and J. R. Reynolds, *Adv. Funct. Mater.*, 2012, **22**, 4801–4813.
11 W. Elsawy, C.-L. Lee, S. Cho, S.-H. Oh, S.-H. Moon, A. Elbarbary and J.-S. Lee, *Phys. Chem. Chem. Phys.*, 2013, **15**, 15193–15203.
12 Y. Ren, A. K. Hailey, A. M. Hiszpanski and Y.-L. Loo, *Chem. Mater.*, 2014, **26**, 6570–6577.
13 T. Wang, Y. Chen, X. Bao, Z. Du, J. Guo, N. Wang, M. Sun and R. Yang, *Dyes Pigments*, 2013, **98**, 11–16.
14 N. M. Randell, A. F. Douglas and T. L. Kelly, *J. Mater. Chem. A*, 2013, **2**, 1085–1092.
15 A. Yassin, P. Leriche, M. Allain and J. Roncali, *New J. Chem.*, 2013, **37**, 502–507.
16 M. Karakawa and Y. Aso, *RSC Adv.*, 2013, **3**, 16259–16263.
17 M. Yang, X. Chen, Y. Zou, C. Pan, B. Liu and H. Zhong, *J. Mater. Sci.*, 2012, **48**, 1014–1020.
18 S. M. McAfee, J. M. Topple, A.-J. Payne, J.-P. Sun, I. G. Hill and G. C. Welch, *ChemPhysChem*, 2014, DOI: 10.1002/cphc.201402662
19 J. E. Coughlin, Z. B. Henson, G. C. Welch and G. C. Bazan, *Acc. Chem. Res.*, 2014, **47**, 257–270.
20 V. Gupta, A. K. K. Kyaw, D. H. Wang, S. Chand, G. C. Bazan and A. J. Heeger, *Sci. Rep.*, 2013, **3**, 1965
21 Y. Sun, G. C. Welch, W. L. Leong, C. J. Takacs, G. C. Bazan and A. J. Heeger, *Nat. Mater.*, 2012, **11**, 44–48.
22 T. S. van der Poll, J. A. Love, T.-Q. Nguyen and G. C. Bazan, *Adv. Mater.*, 2012, **24**, 3646–3649.
23 Y. Chen, X. Wan and G. Long, *Acc. Chem. Res.*, 2013,46, 2645–2655.
24 A. Mishra and P. Bäuerle, *Angew. Chem. Int. Ed.*, 2012, **51**, 2020–2067.
25 G. C. Welch, L. A. Perez, C. V. Hoven, Y. Zhang, X.-D. Dang, A. Sharenko, M. F. Toney, E. J. Kramer, T.-Q. Nguyen and G. C. Bazan, *J. Mater. Chem.*, 2011, **21**, 12700–12709.
26 H.-J. Yun, G. B. Lee, D. S. Chung, Y.-H. Kim and S.-K. Kwon, *Adv. Mater.*, **2014**, *26*, 6612-6616.
27 J.-H. Chang, H.-F. Wang, W.-C. Lin, K.-M. Chiang, K.-C. Chen, W.-C. Huang, Z.-Y. Huang, H.-F. Meng, R.-M. Ho and H.-W. Lin, *J. Mater. Chem. A*, 2014, **2**, 13398–13406.
28 W. Kang, M. Jung, W. Cha, S. Jang, Y. Yoon, H. Kim, H. J. Son, D.-K. Lee, B. Kim and J. H. Cho, *ACS Appl. Mater. Interfaces*, 2014, **6**, 6589–6597.
29 A. Zhugayevych, O. Postupna, R. C. Bakus II, G. C. Welch, G. C. Bazan and S. Tretiak, *J. Phys. Chem. C*, 2013, **117**, 4920–4930.
30 C. J. Takacs, Y. Sun, G. C. Welch, L. A. Perez, X. Liu, W. Wen, G. C. Bazan and A. J. Heeger, *J. Am. Chem. Soc.*, 2012, **134**, 16597–16606.
31 J. K. Lee, W. L. Ma, C. J. Brabec, J. Yuen, J. S. Moon, J. Y. Kim, K. Lee, G. C. Bazan and A. J. Heeger, *J. Am. Chem. Soc.*, 2008, **130**, 3619–3623.

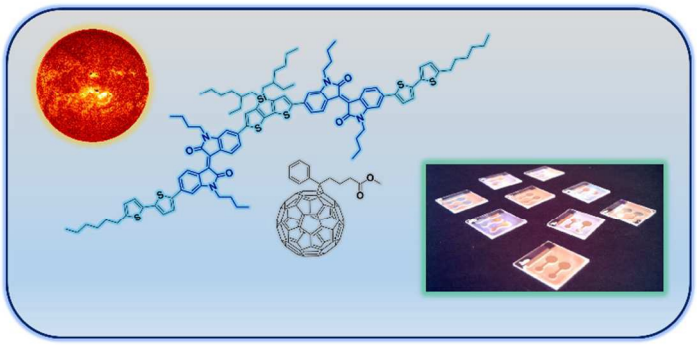

Organic photovoltaics devices with 3.2% PCE were demonstrated using an isoindigo small molecule donor: fullerene acceptor active layer.